ORIGINAL RESEARCH

MiR-27b-3p facilitates non-small cell lung cancer cell ferroptosis through targeting SLC7A11

Rong Chen[1], Qingyu Zhou[2], Shuai Guo[1], Yahui Shen[1,*]

1. Department of Respiratory and Critical Care Medicine, The Affiliated Taizhou People's Hospital of Nanjing Medical University, Taizhou School of Clinical Medicine, Nanjing Medical University, Taizhou, Jiangsu 225300, China.
2. Taizhou School of Clinical Medicine, Nanjing Medical University, Taizhou, Jiangsu 225300, China.

*** Corresponding Author:Yahui Shen**; E-mail: shenyahui@njmu.edu.cn

Abstract

Objective

To investigate the role of microRNA-27b-3p (miR-27b-3p) in regulating ferroptosis in non-small cell lung cancer (NSCLC) cells and to elucidate the underlying molecular mechanism, with a focus on its interaction with SLC7A11.

Methods

The expression levels of miR-27b-3p and SLC7A11 were examined in NSCLC cell lines. Gain-of-function experiments were performed by overexpressing miR-27b-3p to assess its effects on NSCLC cell proliferation, migration, invasion, apoptosis, and ferroptosis. Ferroptosis was evaluated by measuring intracellular free iron, lipid peroxidation, and reactive oxygen species (ROS) levels in erastin-treated NSCLC cells. The targeting relationship between miR-27b-3p and SLC7A11 was analyzed, and rescue experiments were conducted by overexpressing SLC7A11 in miR-27b-3p–overexpressing cells.

Results

miR-27b-3p expression was significantly downregulated, while SLC7A11 expression was upregulated in NSCLC cells. Overexpression of miR-27b-3p inhibited NSCLC cell proliferation, migration, and invasion, and enhanced apoptosis and ferroptosis, as indicated by increased free iron, lipid peroxidation, and ROS levels in erastin-treated cells. SLC7A11 was identified as a target of miR-27b-3p, and its overexpression reversed the inhibitory effects of miR-27b-3p on proliferation, migration, and invasion, as well as the promoting effects on apoptosis and ferroptosis in NSCLC cells.

Conclusion

miR-27b-3p acts as a tumor suppressor in NSCLC by inducing ferroptosis and inhibiting malignant behaviors of NSCLC cells through direct targeting and negative regulation of SLC7A11. These findings suggest that the miR-27b-3p/SLC7A11 axis may represent a potential therapeutic target for NSCLC.

Keywords: non-small cell lung cancer, ferroptosis, miR-27b-3p, SLC7A11

Introduction

In 2020, the global landscape of lung cancer was marked by around 2.2 million newly diagnosed cases as well as around 1.8 million deaths linked to this disease[1]. These figures account for 11.4 percentage of all cancer incidences as well as 18.0 percentage of cancer-related mortalities, respectively[2]. Beyond tobacco consumption, the onset of lung cancer is also influenced by environmental and occupational exposures, chronic pulmonary conditions, as well as various lifestyle choices[3]. Non-small cell lung cancer (NSCLC) occupies roughly 85 percentage of all lung cancer diagnoses[4]. Treatment strategies for NSCLC, tailored to the patient's clinical presentation, encompass surgery, chemical therapy, radiation treatment, targeted therapy, as well as immune therapy, each offering substantial benefits to patients[5]. Despite these advancements, the overall survival rate for NSCLC patients presents dishearteningly poor spanning from 68 percentage for individuals with stage IB to less than 10 percentage for those with stages IVA-IVB. This poor prognosis is primarily attributed to distant metastasis, local recurrence, as well as the emergence of drug resistance[6]. To enhance survival outcomes for NSCLC patients, it is essential to delve deeper into the pathological mechanisms driving NSCLC progression and to discover novel molecular targets for therapeutic intervention.

Ferroptosis represents a recently emerged concept within the field of programmed cell death, distinguishing itself from other forms such as apoptosis, necroptosis, and pyroptosis through its unique morphological characteristics, notably the shrinkage of mitochondrial size and a decrease in cristae[7]. Initially investigated in mammalian systems, ferroptosis has since gained recognition as a prevalent and pivotal mechanism of cellular destruction[8]. Ferroptosis is characterized by an elevation in reactive oxygen species (ROS) levels and widespread lipid peroxidation within cells[9]. These biochemical transformations induce significant modifications in mitochondrial function and architecture, coupled with an increase in mitochondrial membrane density[10]. Within this cellular milieu, intracellular $Fe2+$ plays a pivotal role through catalyzing the peroxidation reaction of unsaturated fatty acids in the cell membrane, ultimately driving the cell towards death[11]. However, the regulatory mechanisms governing ferroptosis in NSCLC remain an area ripe for further investigation.

MicroRNAs (miRNAs) are diminutive noncoding RNAs, typically comprising around 25 nucleotides, that modulate gene expression through combining with target mRNAs' 3'-untranslated region (UTR). Numerous literatures have underscored the participation of miRNAs in NSCLC progression[12]. Likewise, miR-3074-5p hampers NSCLC advancement by targeting the YWHAZ/Hsp27 signaling axis[13]. Conversely, certain miRNAs function as oncogenes in NSCLC. Notably, miRNA-20a-5p has been documented to bolster NSCLC cell invasion by targeting KLF9[14]. Additionally, microRNA-92a has been discovered to accelerate NSCLC cell proliferation by targeting FBXW7[15]. Despite these revelations, the precise roles of miRNAs in NSCLC along with the underlying molecular mechanisms through which they exert their effects on this cancer type remain predominantly uncharted territory, warranting further exploration.

MiR-27b-3p, recognized as a promising tumor suppressor, frequently exhibits reduced expression across a spectrum of human malignancies. For instance, miR-27b-3p attenuates colorectal cancer cell proliferation and migration[16]. Similarly, it exerts inhibitory effects on proliferation and holds the potential to reverse multidrug resistance in breast cancer cells[17]. Notably, reports have also suggested miR-27b-3p is low-expressed in NSCLC cells, where it suppresses cell proliferation, migration, as well as invasion[18]. Nevertheless, miR-27b-3p's role in modulating ferroptosis within NSCLC, along with the underlying mechanisms, remain elusive.

In our study, we set out to elucidate miR-27b-3p's role in regulating ferroptosis in NSCLC, as well as to unravel the specific molecular pathways involved.

Material and methods

Cell culture and treatment

Procell, China provided BEAS-2B as well as several NSCLC cell lines (A549, H1299, NCI-H520, and SK-MES-1). DMEM (BEAS-2B), Ham's F-12K medium (A549), RPMI-1640 medium (H1299 and NCI-H520), and Minimal Essential Medium (SK-MES-1) were fortified with 10% fetal bovine serum (FBS) and 1% penicillin/streptomycin, and cultivated at 37°C with 5% CO2. To trigger ferroptosis, cells were exposed to erastin (20 μM) for 24 hours, based on established protocols from prior studies[19].

Cell transfection

RiboBio, China supplied miR-27b-3p mimics and pcDNA3.1-SLC7A11, along with their respective negative controls (NC mimics and pcDNA3.1). Once the cells in 6-well plates reached 80% confluence, 1×10^6 cells per well were transfected utilizing Lipofectamine 2000 reagent.

RT-qPCR

Utilizing TRIzol reagent, total RNA was extracted from cells. After extraction, the isolated RNA was reversely transcribed into cDNA utilizing a First Strand cDNA Synthesis Kit. Subsequently, RT-qPCR was implemented with a SYBR Premix ExTaq Reverse Transcription PCR kit. Gene expression levels were relatively quantified by normalizing against U6 and GAPDH, applying the 2□ΔΔCt method. The primer sequences are detailed in Table 1.

Western blot analysis

Cells were lysed utilizing RIPA buffer (Sigma-Aldrich, USA). Following determining the protein concentration, proteins were isolated by SDS-PAGE on 8% gels and transferred onto PVDF membranes (Millipore, USA). Following being blocked with 5% non-fat milk, the membranes were cultivated with primary antibodies at 4°C for one night. Next, the membranes were subjected to cultivate with HRP-conjugated secondary antibodies (1:2000, ab6721, Abcam, UK) for 1 hour at 25°C. Protein bands were visualized utilizing an ECL Advance reagent. The dilution ratios and catalog numbers of the primary antibodies are provided in Table 2.

CCK-8

After transfection, cells were subjected to seed into 96-well plates. Subsequently, CCK-8 reagent was subjected to add into each well at 24-hour, 48-hour, and 72-hour intervals, followed by incubation for 2 hours. The optical density at 450 nm was measured by means of a microplate reader.

Colony formation

After transfection, the cells (1 × 105 cells per well) were subjected to seed into 6-well plates. Subsequently, they were incubated for 10 days. Next, the colonies were fixed and stained, followed by counting the number of colonies.

Flow cytometry

We employed Annexin V-FITC/PI apoptosis detection kits (Yeasen, China) to evaluate cell apoptosis. Following the completion of transfection, the cells were detached using trypsin and subsequently centrifuged. Next, Annexin V-FITC solution (5 μl) and PI solution (10 μl) were introduced to the cells, which were then incubated in the absence of light at 25°C for 10 minutes. Ultimately, a flow cytometer was utilized for analyzing cell apoptosis rate.

Transwell

To evaluate cell migration and invasion, Transwell inserts (Corning, USA) featuring membranes with 8-μm pores were employed. In the migration assay, the lower chamber was loaded with 800 μl of medium which comprised 10% FBS. Then, cells suspended in 200 μL of medium which comprised 1% FBS were introduced into the upper chamber and cultivated at 37°C for a duration of 24 hours. The migrated cells were then fixed and dyed. Microscopic images were captured, and the count of migrated cells was determined. For assessing cell invasion, the inserts were initially coated with Matrigel. The subsequent steps mirrored those of the migration assay.

Malondialdehyde (MDA) assay

The level of malondialdehyde (MDA) in cell lysates was determined utilizing a Lipid Peroxidation Assay Kit. The concentration was subsequently quantified through colorimetric measurement at an optical density (OD) of 532 nm.

Iron assay

The intracellular ferrous iron (Fe2+) was measured utilizing an Iron Assay Kit. Cells were seeded in 10 cm² dish for one night. Subsequently, the cells were gathered, homogenized, and centrifuged. The resulting supernatant was mixed with a reagent which contained iron reductase. After a 40-minute incubation period, the optical density was assessed at 593 nm by means of a microplate reader.

Lipid ROS measurement

Lipid ROS levels were evaluated by flow cytometry employing BODIPY-C11 dye (Thermo Fisher Scientific, USA). Initially, cells were subjected to seed in a 6-well plate and cultured for one night. Following this, the cells were subjected to treat with either erastin or DMSO for 24 hours. Next, the cells were stained with 5 μM BODIPY-C11 and incubated without light at 37 °C for 20 minutes. The intracellular lipid ROS levels were quantified via flow cytometry. The resulting data were analyzed using FlowJo Software.

Dual-luciferase reporter gene assay

Luciferase assays were conducted by means of the pmiR-GLO Dual Luciferase Reporter System (Promega, USA). Specifically, the sequences of miR-27b-3p, along with the wild-type (WT) or mutant (MUT) versions of the SLC7A11 3'UTR, were cloned into the pmiR-GLO plasmid. Subsequently, cells were co-transfected with either the WT or MUT plasmid, along with miR-27b-3p mimics or NC mimics, by means of Lipofectamine 2000. Forty-eight hours post-transfection, luciferase activity was measured utilizing the Dual-Luciferase Assay Kit (Promega, USA).

RNA pull-down assay

An RNA pull-down assay was implemented by means of the Magnetic RNA Pull-Down Kit sourced from Pierce, USA. Briefly, biotin-labeled miR-27b-3p and bio-NC probes were mixed with magnetic beads, followed by cultivating with the isolated total RNA. After elution, the enrichment of RNA was analyzed via RT-qPCR.

Statistical analysis

Data analysis was performed by means of SPSS 13.0 software. Data were expressed as the mean ± standard deviation (SD) from three independent experiments. Statistical comparisons were conducted using a Student's t-test or one-way analysis of variance (ANOVA) followed by Tukey's post-hoc test. A P-value < 0.05 was considered statistically significant.

Results

MiR-27b-3p is downregulated in NSCLC cell malignant behaviors

As revealed in Figure 1A, miR-27b-3p expression was significantly lower in four NSCLC cell lines relative to the BEAS-2B cell line. Since miR-27b-3p levels were particularly diminished in A549 and H1299 cell lines relative to the other NSCLC cell lines, these two were selected for subsequent investigations. Figure 1B revealed a marked elevation in miR-27b-3p levels in NSCLC cells following miR-27b-3p mimics transfection. In CCK-8 assays, we observed that overexpressed miR-27b-3p caused a substantial decrease in NSCLC cell viability compared to those transfected with NC mimics (Figure 1C). Colony formation assays demonstrated a decline in the number of cell colonies in NSCLC cells with miR-27b-3p elevation (Figure 1D). Flow cytometry analysis demonstrated that miR-27b-3p elevation significantly boosted the apoptosis rate of NSCLC cells in comparison to the NC inhibitor group (Figure 1E). Moreover, miR-27b-3p overexpression induced a notable increase in the levels of pro-apoptotic proteins (cleaved caspase-3 and Bax), while concurrently reducing the levels of the anti-apoptotic protein (Bcl-2) (Figure 1F). Transwell assays manifested that upregulated miR-27b-3p impeded cell migration and invasion (Figure 1G-1H).

MiR-27b-3p promotes ferroptosis in erastin-induced NSCLC cells

Erastin is a small molecule compound known to trigger ferroptosis 20.Upon administering erastin to NSCLC cells, we observed cell death in NSCLC cells.

However, the survival rate of NSCLC cells transfected with miR-27b-3p mimics was notably lower relative to those with NC mimics (Figure 2A). Lipid peroxidation and iron accumulation are crucial signaling events that initiate ferroptosis 21. MDA is a key end-product of lipid peroxidation 22, prompting us to examine whether miR-27b-3p influences MDA accumulation in NSCLC cells. As depicted in Figure 2B, upon miR-27b-3p elevation, the erastin-induced MDA levels were significantly amplified even further. Likewise, miR-27b-3p overexpression led to an enhanced production of lipid ROS in NSCLC cells subjected to erastin treatment (Figure 2C). Given that Fe2+ has a pivotal role in the execution of ferroptosis 23, we further found that upon erastin treatment, intracellular Fe2+ concentrations increased in NSCLC cells. Remarkably, miR-27b-3p overexpression caused an additional surge in intracellular Fe^{2+} levels (Figure 2D).

MiR-27b-3p negatively regulates SLC7A11 in NSCLC cells

By utilizing the starBase website, we identified that miR-27b-3p possesses the capability to target SLC7A11 mRNA 3'UTR (Figure 3A). SLC7A11 is instrumental in governing ferroptosis, as it promotes the uptake of cysteine necessary for glutathione synthesis and antioxidant defense, thereby exerting a negative regulatory effect on ferroptosis [24]. Based on this, we postulated that miR-27b-3p might augment NSCLC cell ferroptosis by regulating SLC7A11. Dual-luciferase reporter assays manifested that miR-27b-3p elevation notably diminished luciferase activity in the SLC7A11 3'UTR-WT group (Figure 3B). Subsequent validation via RNA pull-down assays demonstrated a substantial enrichment of SLC7A11 in the group treated with biotin-labeled miR-27b-3p (Figure 3C). We further discovered that overexpressing miR-27b-3p reduced SLC7A11 levels in NSCLC cells (Figure 3D-3E). Lastly, we confirmed that SLC7A11 expression was significantly elevated in NSCLC cells (Figure 3F).

MiR-27b-3p represses NSCLC cell malignant behaviors by modulating SLC7A11 expression

Whether miR-27b-3p's antiproliferative and pro-apoptotic effects were mediated

Table 1 Primer sequences for RT-qPCR

Gene	Forward (5'-3')	Reverse (5'-3')
miR-27b-3p	TTATGCCCAGCGATGACC	GGCTCCAACTTAACTGTCCC
SLC7A11	GGCTCCATGAACGGTGGTGTG	GCTGGTAGAGGAGTGTGCTTGC
GAPDH	GAAGATGGTGATGGGATTTC	AACGCTTCACGAATTTGCGT
U6	CTCGCTTCGGCAGCACA	GTCATACTCCTGCTTGCTGAT

Table 2 Dilution and catalogue of primary antibodies

Protein	Dilution	Catalogue	Manufacturer
Cleaved caspase-3	1:500	ab32042	Abcam, UK
Bax	1:1000	ab32503	Abcam, UK
Bcl-2	1:2000	ab182858	Abcam, UK
SLC7A11	1:1000	ab307601	Abcam, UK
GAPDH	1:2500	ab9485	Abcam, UK

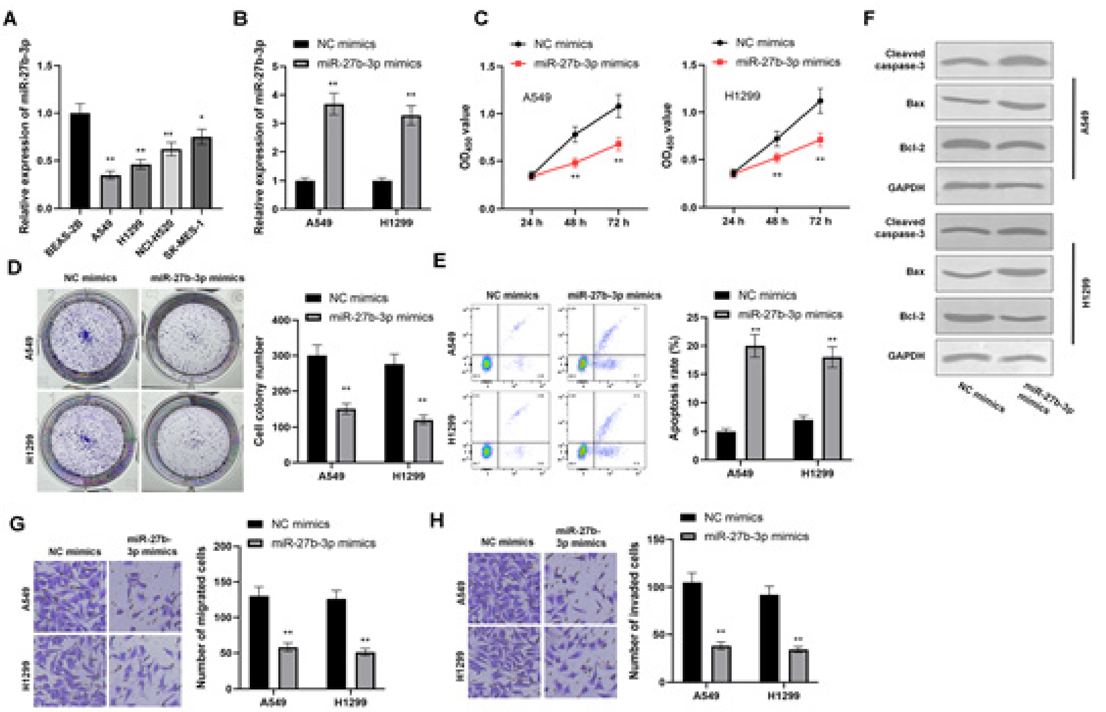

Figure 1 MiR-27b-3p is upregulated in NSCLC cells and promotes cell proliferation, migration and invasion in NSCLC. (A) MiR-27b-3p expression was determined by RT-qPCR in NSCLC cell lines and normal bronchial epithelial cell line BEAS-2B. (B) MiR-27b-3p expression was measured by RT-qPCR after miR-27b-3p mimics transfection. (C) The effect of miR-27b-3p overexpression on NSCLC cell viability were examined using CCK-8 assays. (D) The effect of miR-27b-3p overexpression on the cell colony number in NSCLC cells were examined using colony formation assays. (E) Flow cytometry analysis of NSCLC cell apoptosis after miR-27b-3p overexpression. (F) Protein expression levels of Cleaved caspase-3, Bcl-2 and Bax in NSCLC cells transfected with miR-27b-3p mimics were measured by western blot analysis. (G-H) Transwell assays of NSCLC cell migration and invasion after miR-27b-3p overexpression. *P<0.05, **P<0.01.

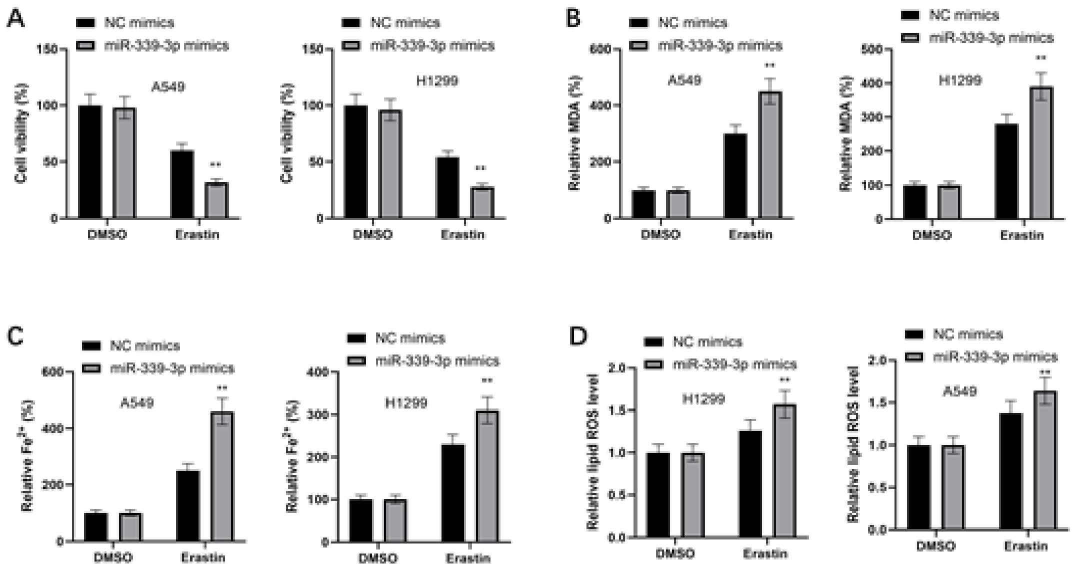

Figure 2 MiR-27b-3p promotes ferroptosis in Erastin-induced NSCLC cells. (A) The cell viability of NSCLC cells transfected with miR-27b-3p mimics was determined using CCK-8 assay in the presence of erastin or DMSO. (B) The lipid formation was measured by MDA assay in NSCLC cells transfected with miR-27b-3p mimics in the presence of erastin or DMSO. (C) Fe2+ accumulation in NSCLC cells transfected with miR-27b-3p mimics in the presence of erastin or DMSO. (D) The lipid ROS level in NSCLC cells transfected with miR-27b-3p mimics was assessed by BODIPY-C11 staining in the presence of erastin or DMSO. **P<0.01.

through the regulation of SLC7A11 was further explored. Initially, the efficiency of pcDNA3.1-SLC7A11 transfection was verified using RT-qPCR and western blot techniques. As a result, transfection with pcDNA3.1-SLC7A11 significantly increased FBXW7 levels compared to pcDNA3.1 transfection in NSCLC cells (Figure 4A-4B). Subsequently, NSCLC cells were co-transfected with miR-27b-3p mimics and pcDNA3.1-SLC7A11. As depicted in Figure 4C-4D, the reduced cell viability and colony formation in NSCLC cells modulated by miR-27b-3p elevation were reversed following co-transfection with pcDNA3.1-SLC7A11. Additionally, overexpressed SLC7A11 counteracted the increased apoptosis rate induced by miR-27b-3p elevation in NSCLC cells (Figure 4E). Furthermore, the elevated levels of Cleaved caspase-3 and Bax, along with the diminished

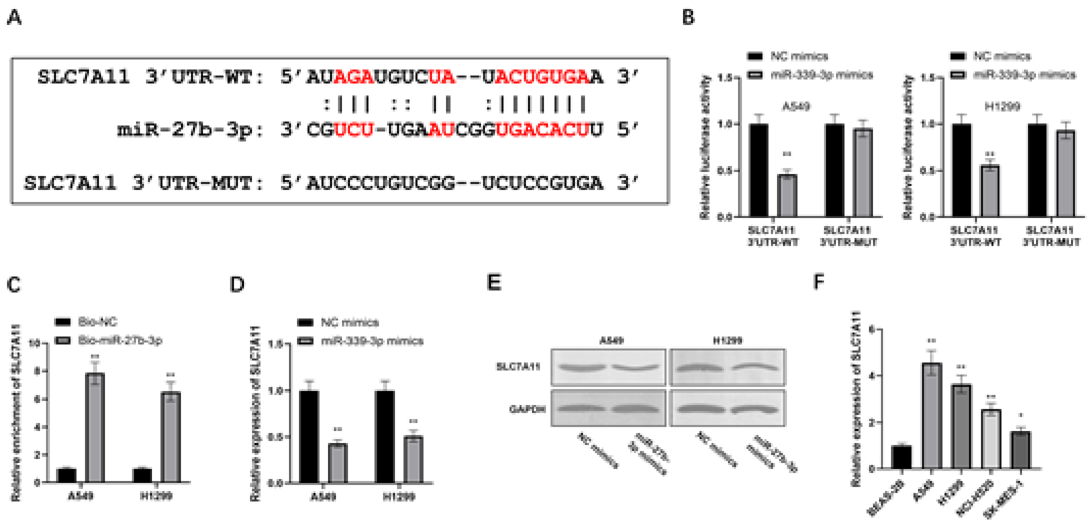

Figure 3 MiR-27b-3p negatively regulates SLC7A11 in NSCLC cells. (A) Binding sites between miR-27b-3p and SLC7A11 3'UTR. (B) Dual-luciferase reporter gene assay measured the relative luciferase activity of SLC7A11 3'UTR-WT/MUT in NSCLC cells transfected with miR-27b-3p mimics. (C) RNA pull-down assay detected the binding between miR-27b-3p and SLC7A11. (D-E) RT-qPCR and western blot analyzed SLC7A11 mRNA and protein expression in NSCLC cells transfected with miR-27b-3p mimics. (F) SLC7A11 expression was determined by RT-qPCR in NSCLC cell lines and normal bronchial epithelial cell line BEAS-2B. *P<0.05, **P<0.01.

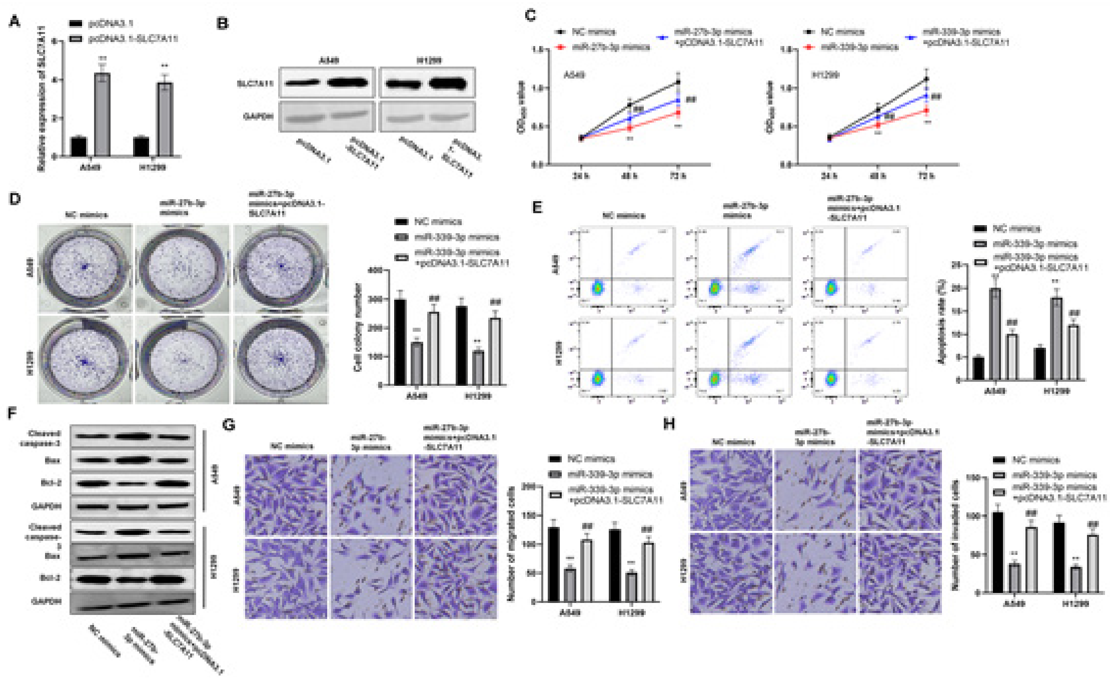

Figure 4 MiR-27b-3p represses cell proliferation, migration and invasion in NSCLC by targeting SLC7A11. (A-B) SLC7A11 expression was measured by RT-qPCR and western blot after pcDNA3.1-SLC7A11 transfection. (C) Cell viability was examined using CCK-8 assays in NSCLC cells co-transfected with miR-27b-3p mimics and pcDNA3.1-SLC7A11. (D) Cell colony number was assessed in NSCLC cells co-transfected with miR-27b-3p mimics and pcDNA3.1-SLC7A11. (E) Cell apoptosis was assessed by flow cytometry analysis in NSCLC cells co-transfected with miR-27b-3p mimics and pcDNA3.1-SLC7A11. (F) Protein expression levels of Cleaved caspase-3, Bcl-2 and Bax in NSCLC cells co-transfected with miR-27b-3p mimics and pcDNA3.1-SLC7A11 were measured by western blot analysis. (G-H) Transwell assays measured the cell migration and invasion in NSCLC cells co-transfected with miR-27b-3p mimics and pcDNA3.1-SLC7A11. **P<0.01, vs NC mimics; ##P<0.01, vs miR-27b-3p mimics.

Bcl-2 expression in miR-27b-3p mimics-transfected NSCLC cells, were neutralized after co-transfection with pcDNA3.1-SLC7A11 (Figure 4F). Moreover, we found that the increased expression of SLC7A11 mitigated the suppressive effects of miR-27b-3p overexpression on NSCLC cell migration and invasion (Figure 4G-4H).

MiR-27b-3p promotes ferroptosis in erastin-induced NSCLC cells by modulating SLC7A11 expression

Moreover, miR-27b-3p's role in promoting ferroptosis in erastin-induced NSCLC cells through the regulation of SLC7A11 was also assessed. In these cells, the reduction in cell viability caused by miR-27b-3p overexpression was counteracted when pcDNA3.1-SLC7A11 was co-transfected (Figure 5A). At the same time, the increase in MDA levels triggered by miR-27b-3p overexpression was mitigated by SLC7A11 upregulation in erastin-induced NSCLC cells

https://dx.doi.org/10.4314/mmj.v37i5.3

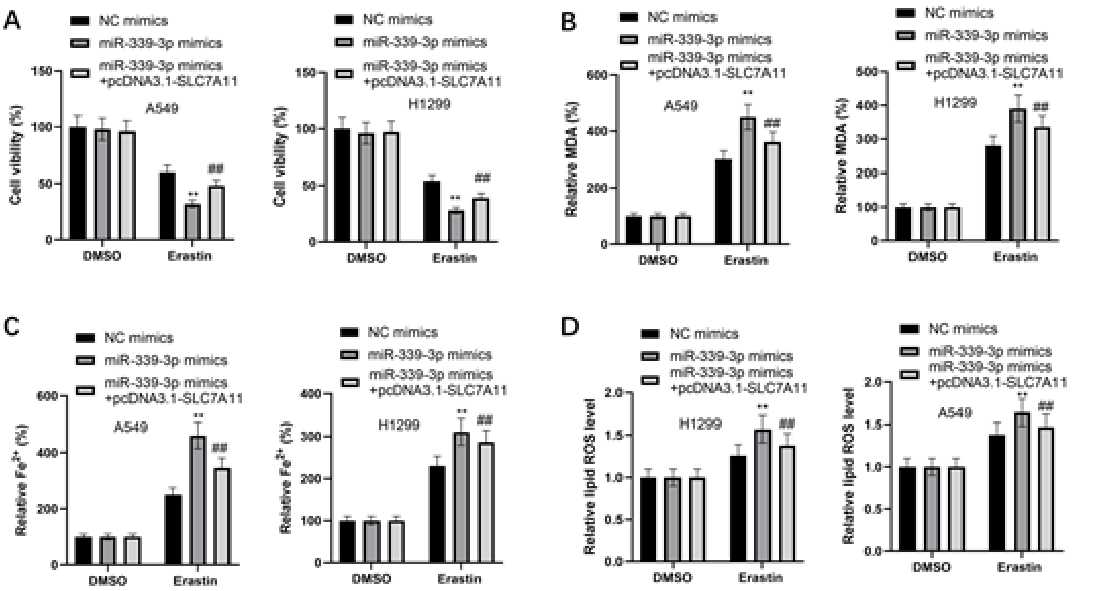

Figure 5 MiR-27b-3p promotes ferroptosis in Erastin-induced NSCLC cells by targeting SLC7A11. (A) The cell viability of NSCLC cells co-transfected with miR-27b-3p mimics and pcDNA3.1-SLC7A11 was determined using CCK-8 assay in the presence of erastin or DMSO. (B) The lipid formation was measured by MDA assay in NSCLC cells co-transfected with miR-27b-3p mimics and pcDNA3.1-SLC7A11 in the presence of erastin or DMSO. (C) Fe2+ accumulation in NSCLC cells co-transfected with miR-27b-3p mimics and pcDNA3.1-SLC7A11 in the presence of erastin or DMSO. (D) The lipid ROS level in NSCLC cells co-transfected with miR-27b-3p mimics and pcDNA3.1-SLC7A11 was assessed by BODIPY-C11 staining in the presence of erastin or DMSO. **P<0.01, vs NC mimics; ##P<0.01, vs miR-27b-3p mimics.

(Figure 5B). Additionally, the rise in Fe2+ levels due to miR-27b-3p upregulation was nullified following pcDNA3.1-SLC7A11 co-transfection (Figure 5C). Furthermore, the heightened lipid ROS levels, which were regulated by miR-27b-3p upregulation, were restored by SLC7A11 upregulation in erastin-induced NSCLC cells (Figure 5D).

Discussion

Finding a way to destroy tumor cells without damaging healthy ones has long been a significant hurdle in cancer therapy. Numerous studies have indicated that ferroptosis is crucial in tumor suppression[24]. This is attributed to the fact that cancer cells require more iron than normal cells[25]. Thus, gaining a deeper insight into the mechanisms that drive ferroptosis could offer new avenues for cancer treatment.

MiR-27b-3p has been implicated in the development of diverse cancers, as evidenced by existing research[26,27]. For instance, miR-27b-3p inhibits the development of esophageal squamous cell carcinoma[28]. Conversely, in triple-negative breast cancer, it accelerates tumor growth[29]. Notably, Sun et al. proposed that miR-27b-3p was low-expressed in lung cancer and functioned as a tumor-suppressive agent[30]. Consistently, this current research revealed miR-27b-3p was significantly downregulated in NSCLC cells. Overexpressed miR-27b-3p substantially repressed NSCLC cell proliferation, migration, along with invasion.

Ferroptosis belongs to a type of programmed cell death that is non-apoptotic and relies on iron and ROS for its execution[31]. Morphologically, ferroptotic cells exhibit mitochondrial structural changes, lack nuclear condensation, and experience plasma membrane rupture, often triggered by the inhibition of system xc-, such as through erastin treatment[32]. In our study, we induced ferroptosis in NSCLC cells using erastin and observed that overexpressed miR-27b-3p elevated levels of free iron, lipid peroxidation, and ROS in these cells. These findings emphasize the pivotal role of miR-27b-3p in regulating ferroptosis.

It is well-known that ferroptosis is tightly regulated by SLC7A11[33]. SLC7A11 belongs to a vital component of the System Xc- system, primarily responsible for transporting cysteine into the cell from the extracellular environment while simultaneously exporting glutamate from the intracellular space[34]. This exchange represents the rate-limiting step in the synthesis of glutathione (GSH), a pivotal molecule for preserving cellular redox homeostasis. Upon entering the cell, cystine is swiftly reduced to cysteine, which serves as an indispensable precursor for GSH production[35]. GSH, functioning as a key cofactor, supplies the reducing equivalents necessary for glutathione peroxidase 4 (GPX4) to operate. GPX4, in turn, plays a vital role in safeguarding cellular integrity by continuously converting toxic lipid peroxides (L-OOH) on the cell membrane into non-toxic lipid alcohols (L-OH). This process effectively shields the cell membrane from oxidative damage and forestalls the onset of ferroptosis[36]. However, when the expression or functionality of SLC7A11 is compromised, it leads to a decline in intracellular cysteine levels and a subsequent depletion of GSH biosynthesis. This depletion indirectly diminishes GPX4 activity, causing the accumulation of lipid peroxides and an exacerbation of ferroptosis within the cells[37]. SLC7A11 is high-expressed in various tumors and is linked to poor patient survival rates[38]. The upregulation of SLC7A11 shields cancer cells from ferroptosis by promoting cystine uptake and GSH synthesis, thereby facilitating tumor development[39]. However, ferroptosis is increasingly recognized as a promising tumor-suppressive mechanism, given its capacity to impede tumor progression by selectively promoting cell death in cancer cells. Since SLC7A11 has a pivotal role in regulating ferroptosis via maintaining cellular redox balance through glutathione synthesis, its inhibition can trigger ferroptosis and potentially suppress tumor progression. As a result, SLC7A11 has garnered significant attention as a possible therapeutic target for cancer[40].

In the current research, miR-27b-3p directly targeted SLC7A11, leading to a significant downregulation of SLC7A11 expression in NSCLC cells. Interestingly, SLC7A11 was observed to be upregulated in NSCLC cells. Notably, when SLC7A11 was overexpressed, it effectively counteracted the repressive impacts of miR-27b-3p elevation on NSCLC cell malignant behaviors. Furthermore, SLC7A11 elevation also attenuated the pro-apoptotic and pro-ferroptotic effects induced by miR-27b-3p in these cells. Likewise, Drayton et al. discovered that decreased miRNA-27a expression affected cisplatin resistance in bladder cancer by targeting SLC7A11[41]. Elrebehy et al. proposed that miR-509-5p facilitated ferroptosis in colorectal cancer cells by targeting SLC7A11[42]. Martino et al. suggested that miR-148a-3p promoted ferroptosis in colorectal cancer cells through targeting SLC7A11[43].

There are certain limitations in our current study. Firstly, we did not carry out in vivo experiments to verify miR-27b-3p's role in regulating resistance in NSCLC. Secondly, we did not investigate the potential signaling pathways influenced by SLC7A11 in NSCLC. Hence, further studies are necessary to gain a more comprehensive comprehension of these mechanisms.

Conclusion

MiR-27b-3p induces NSCLC cell ferroptosis by targeting SLC7A11, providing a novel and promising avenue for the treatment of NSCLC.

References

1.Li C, Lei S, Ding L, Xu Y, Wu X, Wang H, et al. Global burden and trends of lung cancer incidence and mortality. Chin Med J (Engl) 2023; 136 (13): 1583-1590. doi: 10.1097/cm9.0000000000002529.

2.Siegel RL, Miller KD, Wagle NS, Jemal A. Cancer statistics, 2023. CA Cancer J Clin 2023; 73 (1): 17-48. doi: 10.3322/caac.21763.

3.Bade BC, Dela Cruz CS. Lung Cancer 2020: Epidemiology, Etiology, and Prevention. Clin Chest Med 2020; 41 (1): 1-24. doi: 10.1016/j.ccm.2019.10.001.

4.Mithoowani H, Febbraro M. Non-Small-Cell Lung Cancer in 2022: A Review for General Practitioners in Oncology. Curr Oncol 2022; 29 (3): 1828-1839. doi: 10.3390/curroncol29030150.

5.Alexander M, Kim SY, Cheng H. Update 2020: Management of Non-Small Cell Lung Cancer. Lung 2020; 198 (6): 897-907. doi: 10.1007/s00408-020-00407-5.

6.Asselain B, Barrière JR, Clarot C, Vabre JP, Gentil Le Pecq B, Duval Y, et al. Metastatic NSCLC: Clinical, molecular, and therapeutic factors associated with long-term survival. Respir Med Res 2019; 76 38-44. doi: 10.1016/j.resmer.2019.07.001.

7.Jiang X, Stockwell BR, Conrad M. Ferroptosis: mechanisms, biology and role in disease. Nat Rev Mol Cell Biol 2021; 22 (4): 266-282. doi: 10.1038/s41580-020-00324-8.

8.Tang D, Chen X, Kang R, Kroemer G. Ferroptosis: molecular mechanisms and health implications. Cell Res 2021; 31 (2): 107-125. doi: 10.1038/s41422-020-00441-1.

9.Wang B, Wang Y, Zhang J, Hu C, Jiang J, Li Y, et al. ROS-induced lipid peroxidation modulates cell death outcome: mechanisms behind apoptosis, autophagy, and ferroptosis. Arch Toxicol 2023; 97 (6): 1439-1451. doi: 10.1007/s00204-023-03476-6.

10.Li D, Wang Y, Dong C, Chen T, Dong A, Ren J, et al. CST1 inhibits ferroptosis and promotes gastric cancer metastasis by regulating GPX4 protein stability via OTUB1. Oncogene 2023; 42 (2): 83-98. doi: 10.1038/s41388-022-02537-x.

11.Su Y, Zhao B, Zhou L, Zhang Z, Shen Y, Lv H, et al. Ferroptosis, a novel pharmacological mechanism of anti-cancer drugs. Cancer Lett 2020; 483 127-136. doi: 10.1016/j.canlet.2020.02.015.

12.Tan T, Xu XH, Lu XH, Wang XW. MiRNA-200a-3p suppresses the proliferation, migration and invasion of non-small cell lung cancer through targeting IRS2. Eur Rev Med Pharmacol Sci 2020; 24 (2): 712-720. doi: 10.26355/eurrev_202001_20050.

13.Dong N, Gu WW, Yang L, Lian WB, Jiang J, Zhu HJ, et al. MiR-3074-5p suppresses non-small cell lung cancer progression by targeting the YWHAZ/Hsp27 axis. Int Immunopharmacol 2024; 138 112547. doi: 10.1016/j.intimp.2024.112547.

14.Fang QY, Deng QF, Luo J, Zhou CC. MiRNA-20a-5p accelerates the proliferation and invasion of non-small cell lung cancer by targeting and downregulating KLF9. Eur Rev Med Pharmacol Sci 2020; 24 (5): 2548-2556. doi: 10.26355/eurrev_202003_20522.

15.Ni D, Teng J, Cheng Y, Zhu Z, Zhuang B, Yang Z. MicroRNA-92a promotes non-small cell lung cancer cell growth by targeting tumor suppressor gene FBXW7. Mol Med Rep 2020; 22 (4): 2817-2825. doi: 10.3892/mmr.2020.11373.

16.Chen Y, Chen G, Zhang B, Liu C, Yu Y, Jin Y. miR-27b-3p suppresses cell proliferation, migration and invasion by targeting LIMK1 in colorectal cancer. Int J Clin Exp Pathol 2017; 10 (9): 9251-9261.

17.Chen D, Si W, Shen J, Du C, Lou W, Bao C, et al. miR-27b-3p inhibits proliferation and potentially reverses multi-chemoresistance by targeting CBLB/GRB2 in breast cancer cells. Cell Death Dis 2018; 9 (2): 188. doi: 10.1038/s41419-017-0211-4.

18.Sun W, Zhang L, Yan R, Yang Y, Meng X. LncRNA DLX6-AS1 promotes the proliferation, invasion, and migration of non-small cell lung cancer cells by targeting the miR-27b-3p/GSPT1 axis. Onco Targets Ther 2019; 12 3945-3954. doi: 10.2147/ott.S196865.

19.Tai F, Zhai R, Ding K, Zhang Y, Yang H, Li H, et al. Long non-coding RNA lung cancer-associated transcript 1 regulates ferroptosis via microRNA-34a-5p-mediated GTP cyclohydrolase 1 downregulation in lung cancer cells. Int J Oncol 2024; 64 (6): doi: 10.3892/ijo.2024.5652.

20.Wang L, Liu Y, Du T, Yang H, Lei L, Guo M, et al. ATF3 promotes erastin-induced ferroptosis by suppressing system Xc(). Cell Death Differ 2020; 27 (2): 662-675. doi: 10.1038/s41418-019-0380-z.

21.Li X, Meng F, Wang H, Sun L, Chang S, Li G, et al. Iron accumulation and lipid peroxidation: implication of ferroptosis in hepatocellular carcinoma. Front Endocrinol (Lausanne) 2023; 14 1319969. doi: 10.3389/fendo.2023.1319969.

22.Kong P, Yang M, Wang Y, Yu KN, Wu L, Han W. Ferroptosis triggered by STAT1- IRF1-ACSL4 pathway was involved in radiation-induced intestinal injury. Redox Biol 2023; 66 102857. doi: 10.1016/j.redox.2023.102857.

23.Ren Y, Mao X, Xu H, Dang Q, Weng S, Zhang Y, et al. Ferroptosis and EMT: key targets for combating cancer progression and therapy resistance. Cell Mol Life Sci 2023; 80 (9): 263. doi: 10.1007/s00018-023-04907-4.

24.Zeng F, Nijiati S, Tang L, Ye J, Zhou Z, Chen X. Ferroptosis Detection: From Approaches to Applications. Angew Chem Int Ed Engl 2023; 62 (35): e202300379. doi: 10.1002/anie.202300379.

25.Mou Y, Wang J, Wu J, He D, Zhang C, Duan C, et al. Ferroptosis, a new form of cell death: opportunities and challenges in cancer. J Hematol Oncol 2019; 12 (1): 34. doi: 10.1186/s13045-019-0720-y.

26.Yang L, Ruan Y, Chen B, Zhu Y, Xu H. Circ_0001671 regulates prostate cancer progression through miR-27b-3p/BLM axis. Sci Rep 2024; 14 (1): 12181. doi: 10.1038/s41598-024-63068-x.

27. Xia M, Duan LJ, Lu BN, Pang YZ, Pang ZR. LncRNA AFAP1-AS1/miR-27b-3p/VEGF-C axis modulates stemness characteristics in cervical cancer cells. Chin Med J (Engl) 2021; 134 (17): 2091-2101. doi: 10.1097/cm9.0000000000001665.

28.Han M, Li N, Li F, Wang H, Ma L. MiR-27b-3p exerts tumor suppressor effects in esophageal squamous cell carcinoma by targeting Nrf2. Hum Cell 2020; 33 (3): 641-651. doi: 10.1007/s13577-020-00329-7.

29.Shen SJ, Song Y, Ren XY, Xu YL, Zhou YD, Liang ZY, et al. MicroRNA-27b-3p Promotes Tumor Progression and Metastasis by Inhibiting Peroxisome Proliferator-Activated Receptor Gamma in Triple-Negative Breast Cancer. Front Oncol 2020; 10 1371. doi: 10.3389/fonc.2020.01371.

30.Sun Y, Xu T, Cao YW, Ding XQ. Antitumor effect of miR-27b-3p on lung cancer cells via targeting Fzd7. Eur Rev Med Pharmacol Sci 2017; 21 (18): 4113-4123.

31.Li J, Cao F, Yin HL, Huang ZJ, Lin ZT, Mao N, et al. Ferroptosis: past, present and future. Cell Death Dis 2020; 11 (2): 88. doi: 10.1038/s41419-020-2298-2.

32.Xue W, Jian W, Meng Y, Wang T, Cai L, Yu Y, et al. Knockdown of SETD2 promotes erastin-induced ferroptosis in ccRCC. Cell Death Dis 2023; 14 (8): 539. doi: 10.1038/s41419-023-06057-8.

33.Liu GZ, Xu XW, Tao SH, Gao MJ, Hou ZH. HBx facilitates ferroptosis in acute liver failure via EZH2 mediated SLC7A11 suppression. J Biomed Sci 2021; 28 (1): 67. doi: 10.1186/s12929-021-00762-2.

34.Chen SJ, Zhang J, Zhou T, Rao SS, Li Q, Xiao LY, et al. Epigenetically upregulated NSUN2 confers ferroptosis resistance in endometrial cancer via m(5)C modification of SLC7A11 mRNA. Redox Biol 2024; 69 102975. doi: 10.1016/j.redox.2023.102975.

35.Wang C, Liu H, Xu S, Deng Y, Xu B, Yang T, et al. Ferroptosis and Neurodegenerative Diseases: Insights into the Regulatory Roles of SLC7A11. Cell Mol Neurobiol 2023; 43 (6): 2627-2642. doi: 10.1007/s10571-023-01343-7.

36.Feng L, Zhao K, Sun L, Yin X, Zhang J, Liu C, et al. SLC7A11 regulated by NRF2 modulates esophageal squamous cell carcinoma radiosensitivity by inhibiting ferroptosis. J Transl Med 2021; 19 (1): 367. doi: 10.1186/s12967-021-03042-7.

37.Li X, Zhang W, Xing Z, Hu S, Zhang G, Wang T, et al. Targeting SIRT3 sensitizes glioblastoma to ferroptosis by promoting mitophagy and inhibiting SLC7A11. Cell Death Dis 2024; 15 (2): 168. doi: 10.1038/s41419-024-06558-0.

38.Zhang W, Sun Y, Bai L, Zhi L, Yang Y, Zhao Q, et al. RBMS1 regulates lung cancer ferroptosis through translational control of SLC7A11. J Clin Invest 2021; 131 (22): doi: 10.1172/jci152067.

39.Yang J, Zhou Y, Xie S, Wang J, Li Z, Chen L, et al. Metformin induces Ferroptosis by inhibiting UFMylation of SLC7A11 in breast cancer. J Exp Clin Cancer Res 2021; 40 (1): 206. doi: 10.1186/s13046-021-02012-7.

40.Zhang X, Zheng X, Ying X, Xie W, Yin Y, Wang X. CEBPG suppresses ferroptosis through transcriptional control of SLC7A11 in ovarian cancer. J Transl Med 2023; 21 (1): 334. doi: 10.1186/s12967-023-04136-0.

41.Drayton RM, Dudziec E, Peter S, Bertz S, Hartmann A, Bryant HE, et al. Reduced expression of miRNA-27a modulates cisplatin resistance in bladder cancer by targeting the cystine/glutamate exchanger SLC7A11. Clin Cancer Res 2014; 20 (7): 1990-2000. doi: 10.1158/1078-0432.Ccr-13-2805.

42.Elrebehy MA, Abdelghany TM, Elshafey MM, Gomaa MH, Doghish AS. miR-509-5p promotes colorectal cancer cell ferroptosis by targeting SLC7A11. Pathol Res Pract 2023; 247 154557. doi: 10.1016/j.prp.2023.154557.

43.Martino E, Balestrieri A, Aragona F, Bifulco G, Mele L, Campanile G, et al. MiR-148a-3p Promotes Colorectal Cancer Cell Ferroptosis by Targeting SLC7A11. Cancers (Basel) 2023; 15 (17): doi: 10.3390/cancers15174342.